Supplement of Atmos. Chem. Phys., 17, 11707–11726, 2017
https://doi.org/10.5194/acp-17-11707-2017-supplement

Atmospheric Chemistry and Physics
Open Access
EGU

Supplement of

Biomass burning at Cape Grim: exploring photochemistry using multi-scale modelling

Sarah J. Lawson et al.

Correspondence to: Sarah J. Lawson (sarah.lawson@csiro.au)

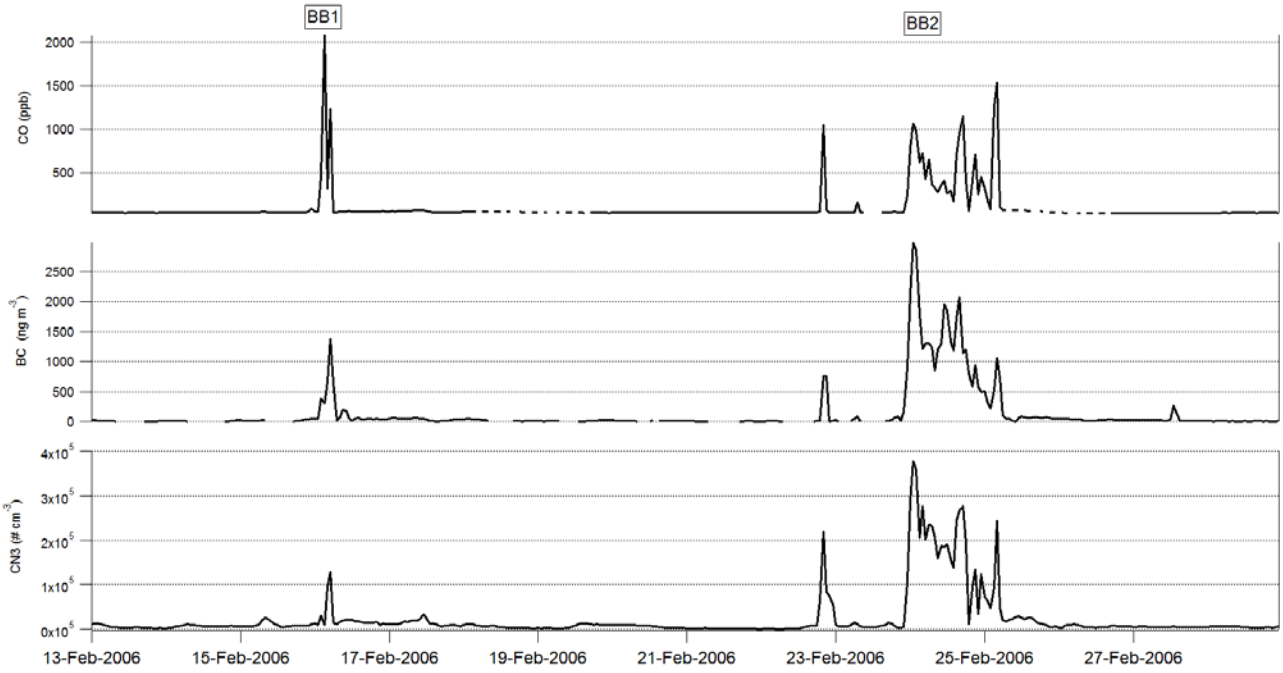

Figure 1. Time series of observed carbon monoxide (CO)- top, black carbon (BC)-middle and particles >3 nm (CN3)-bottom, for the study period. Taken from Lawson et al., 2015.

Performance of the numerical meteorological modelling

The TAPM (Hurley, 2008) and CCAM (McGregor and Dix, 2008) meteorological simulations form an integral component of the analysis presented in our manuscript. As such, it is helpful to undertake qualitative and quantitative comparisons of modelled and observed meteorological parameters in order to assess the relative performance of each model. Although a full assessment of the performance of TAPM and CCAM were beyond the scope of this project (and not supported by a comprehensive set of observational data), we are able to assess model performance for hourly wind, temperature and humidity which were observed at the Cape Grim Base Line monitoring station. The results of a comparison of these data with the simulations of TAPM and CCAM for the period 13–27 February 2006 are summarised below.

Figure 2 shows the scatter plots of observed and modelled wind, temperature and relative humidity and suggest that TAPM performs marginally than CCAM for the 10 m wind speed modelling with a higher coefficient of determination, a better intercept for the least squares regression line of best fit although a 5% lower slope. CCAM has better performance for the modelling of the screen temperature (significantly better slope and intercept), and TAPM performs better for the modelling of relative humidity (note that this parameter also includes the effect of temperature).

Figure 3 shows the sample probability density functions (pdf) for the observation and model wind speed, wind direction, temperature and relative humidity time series. Note that the observed pdfs differ slightly between the TAPM and the CCAM plots because TAPM times are in Australian Eastern Standard while the CCAM plots are in UTC and the sampling periods are slightly different. In the following we consider the qualitative similarities and differences between the observed and modelled pdfs.

Figure 3 (top row) shows that CCAM has better matched the wind speed pdf, with a good representation of the mode at around 9 ms^{-1}. On the other hand TAPM mode occurs at 7 m s^{-1}. Both models simulate a mode in the wind direction pdf for the sector centred on 75^o south (observed mode at 90^o south. TAPM successfully models two modes in the west–south-west sector while CCAM simulates a single mode only (at 225^o). With respect to the screen temperature Figure 2 (third row) shows that CCAM has better simulated the width and peak of the observed temperature pdf, with TAPM under predicting the pdf width and over predicting the peak.

TAPM does a better job of modelling the RH pdf with CCAM under estimating the width of the pdf and overestimating the magnitude of the mode at 90% RH (Figure 3- bottom).

We complete this section by considering a suite of statistical measures of model performance. Figure 4 shows 10 statistical measures- see Hurley et al. (2005), with more details of the metrics given in Willmott (1981) and Thorpe (1985) which can be used to give a quantitative comparison of the TAPM and CCAM 10 m wind speed simulations. Figure 4 (top row) shows that CCAM simulates the campaign mean wind speed to within -14% (thus a low bias) while TAPM has a low bias of 25%. The observed standard deviation of the wind speed is modelled to within -14% by TAPM and 3% by CCAM- see SKILLv in Figure 4 (bottom row). The root mean square error (RMSE) is 2.5 m^{-1} for TAPM and 3.7 m s^{-1} for CCAM. In this regard, a useful measure of skill is the ratio of the RMSE to the observed standard deviation (SKILLr in Figure 4) with SKILLr < 1 being desirable. It can be seen that both models have satisfied this criteria and that TAPM has performed better than CCAM with respect to this metric. Consideration of the RMSE metrics also indicate general good skill from both models, and with TAPM performing better than CCAM. The Index of Agreement (IOA; unity is ideal) also provides evidence of good model performance.

Figure 5 shows the same statistical measures for screen temperature and again indicates skill in the modelling according to the metrics of Willmott (1981) and Thorpe (1985). Again the TAPM performance is slightly better than CCAM. Similar conclusions can be drawn with respect to the relative humidity (Figure 6).

In summary, a necessary condition is that the meteorological models are able to demonstrate reasonable skill in modelling the meteorological conditions within the vicinity of the smoke trajectories as they couple Cape Grim with the smoke source area on Robbin's Island. The information presented above is promising (although not a complete model verification), and does suggest that the TAPM simulations are slightly better than the CCAM simulations with respect to the low level wind, temperatures and relative humidity.

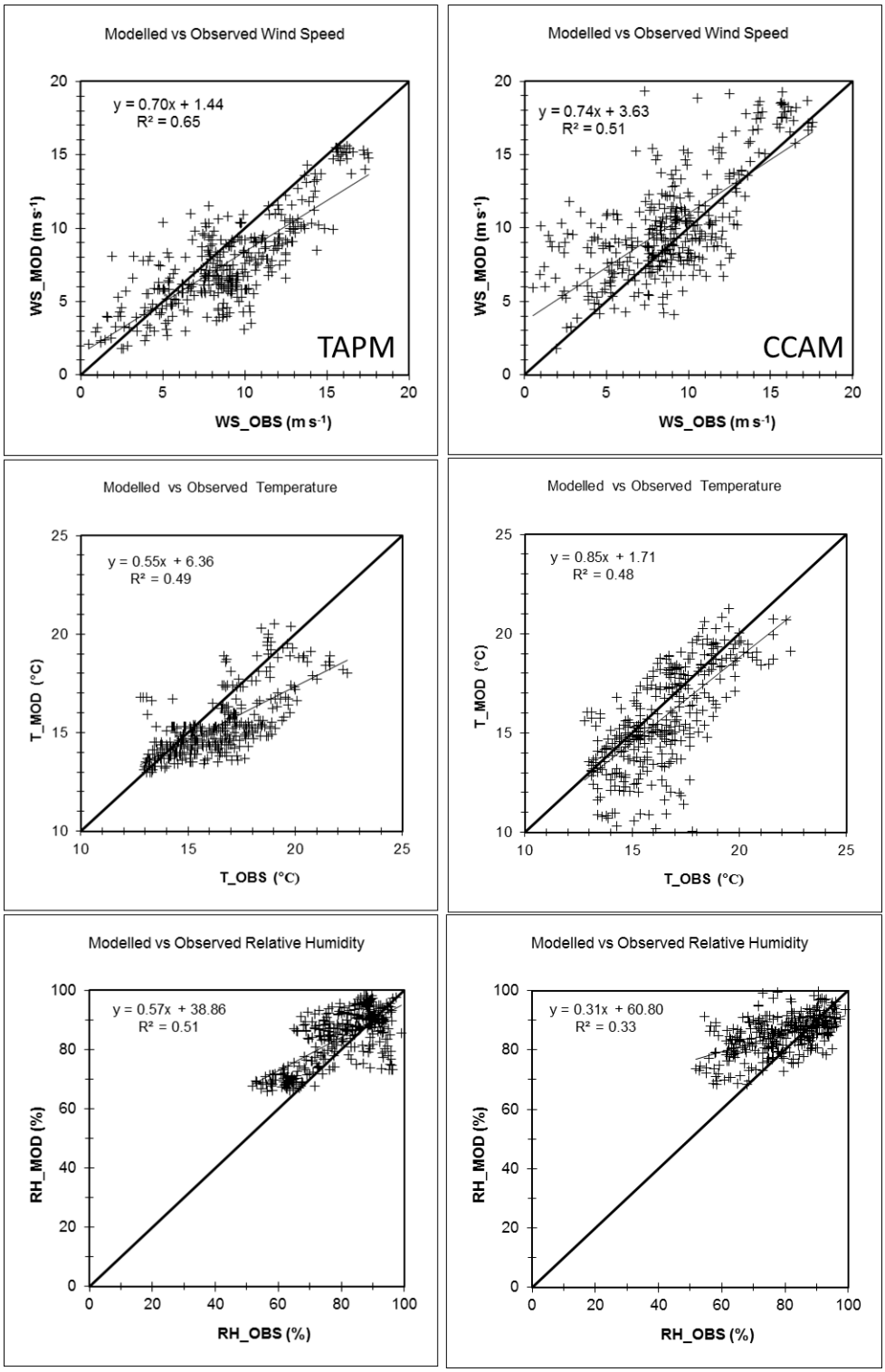

Figure 2. Scatter plots of (by row) observed and modelled 10 m wind speed, screen temperature, relative humidity for (by column). TAPM is shown in the first column and CCAM is shown in the second column.

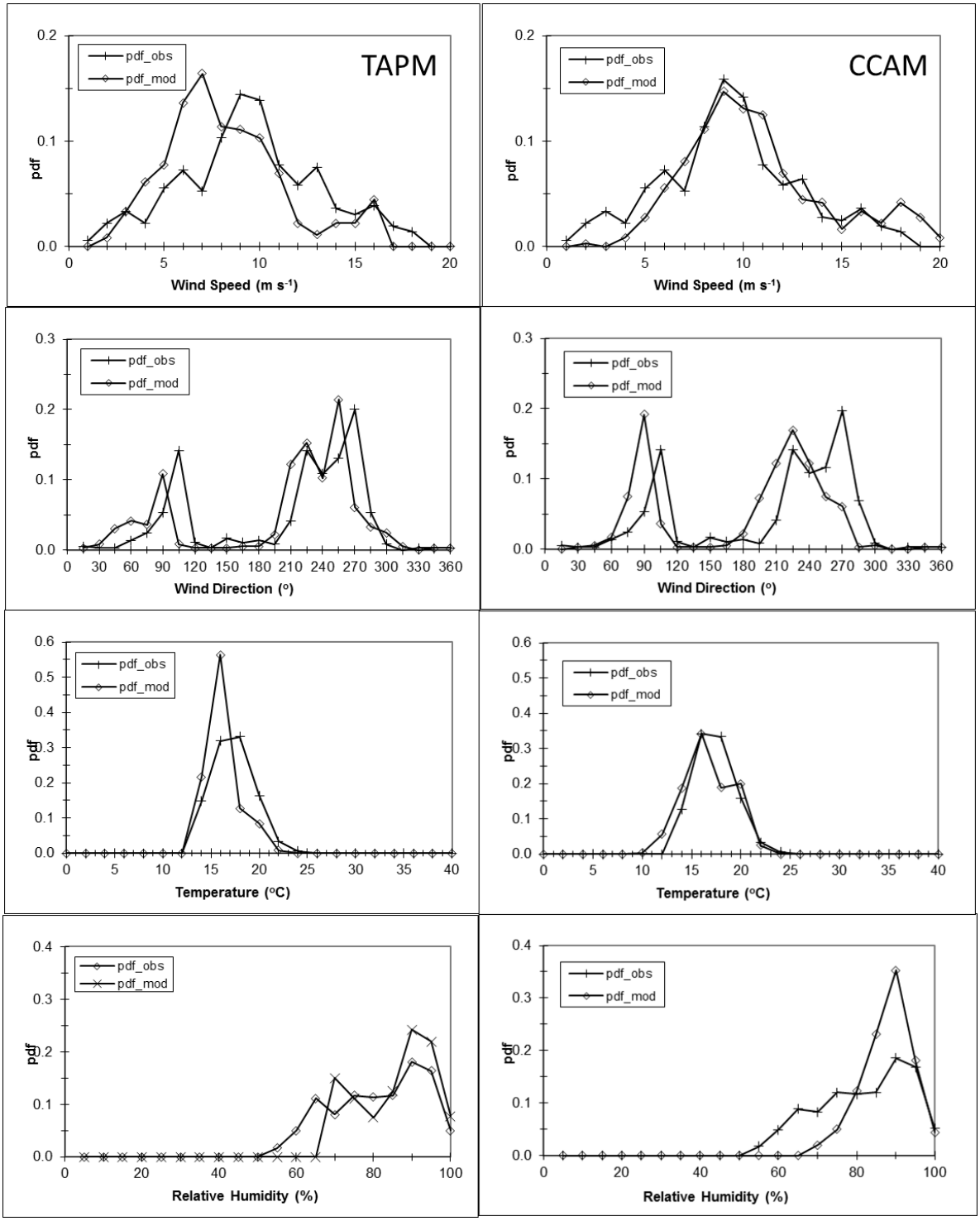

Figure 3. Probability density functions of observed and modelled (by row) 10 m wind speed, 10 m wind direction, screen temperature and screen relative humidity. TAPM results are shown in the first column and CCAM results in the second column.

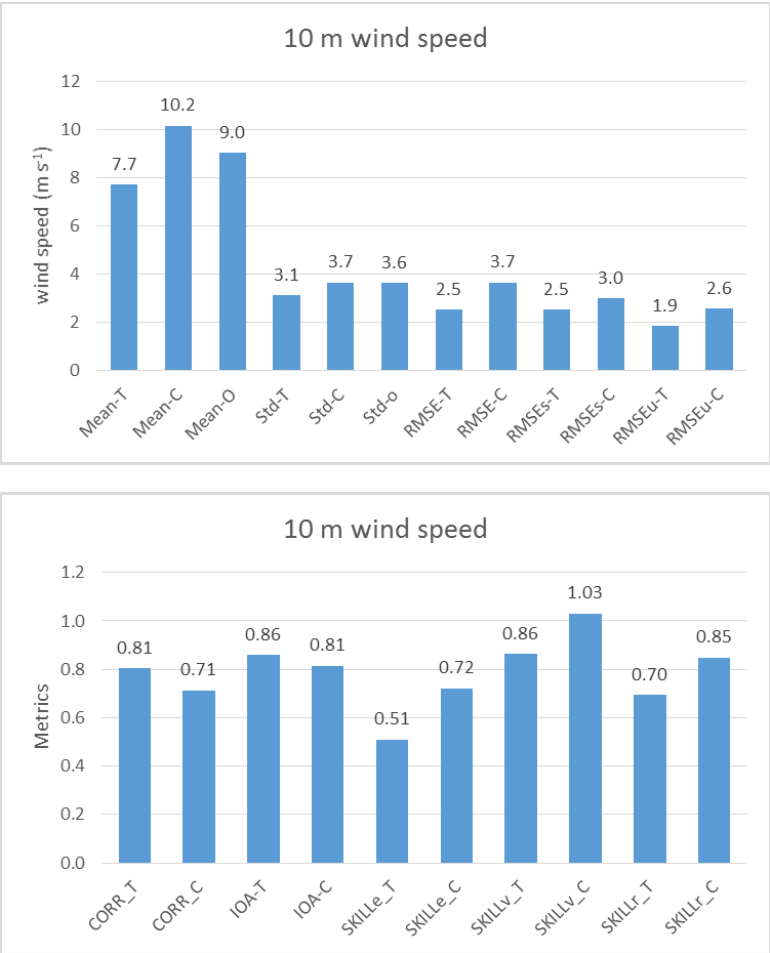

Figure 4. Statistical measures for quantitative comparison of the TAPM and CCAM 10 m wind speed simulations. T=TAPM, C=CCAM, O=Observations. Top- Mean-T, Mean-C, Mean-O; mean TAPM, CCAM and observed 10 m wind speed. Std-T/C standard deviation of the modelled wind (TAPM; CCAM), RMSE- root mean square error; RMSEs- systematic root mean square error; RMSEu- unsystematic root mean square error. Bottom- the metrics are CORR correlation coefficient; IOA- index of agreement; SKILLe = RMSEu/STD-O, SKILLv = Std-model/Std-obs, SKILLr = RMSE/Std-O.

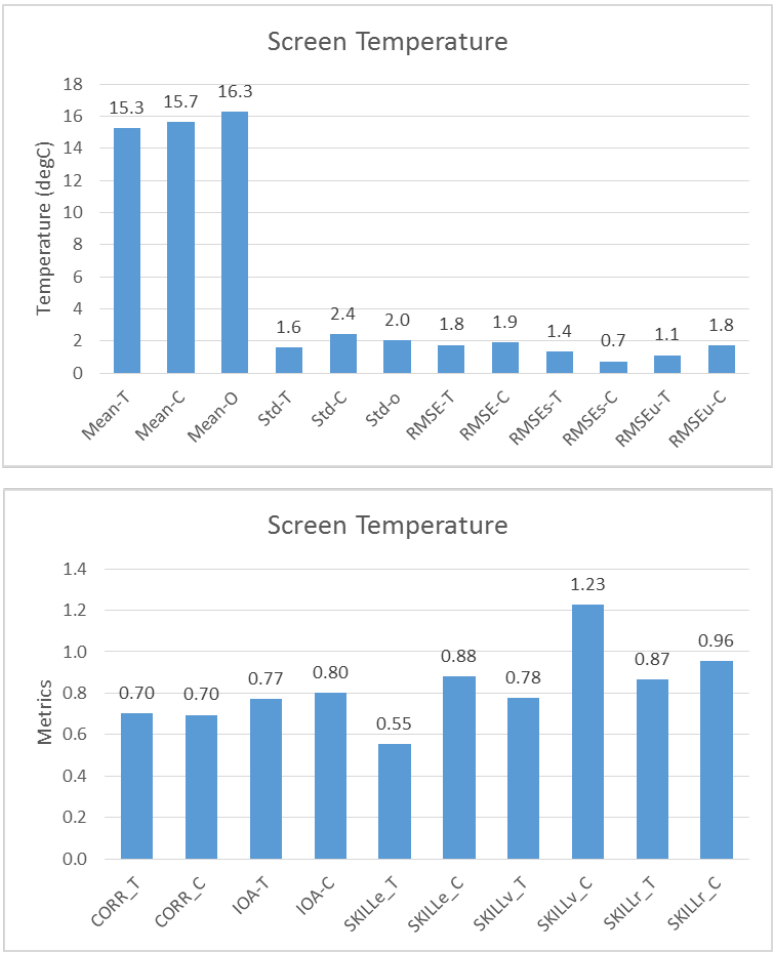

Figure 5. Statistical measures for quantitative comparison of the TAPM and CCAM screen temperature. T=TAPM, C=CCAM, O=Observations. Top- Mean-T, Mean-C, Mean-O; TAPM, CCAM and observed screen temperature. Std-T/C standard deviation of the modelled temperature (TAPM; CCAM), RMSE- root mean square error; RMSEs- systematic root mean square error; RMSEu- unsystematic root mean square error. Bottom- the metrics are CORR correlation coefficient; IOA- index of agreement; SKILLe = RMSEu/STD-O, SKILLv = Std-model/Std-obs, SKILLr = RMSE/Std-O.

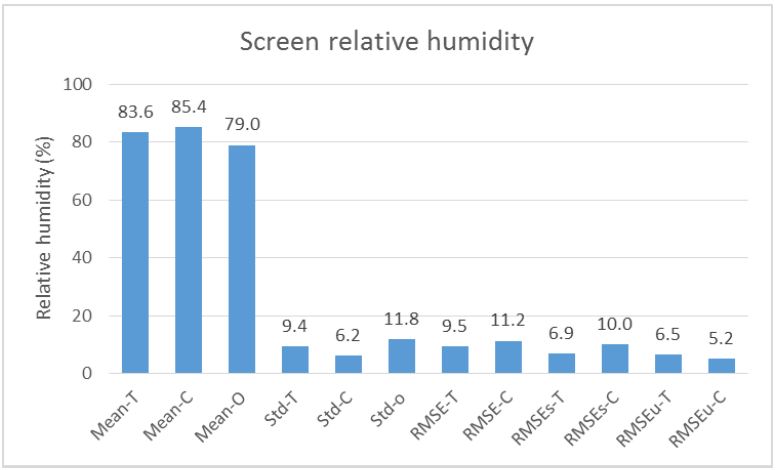

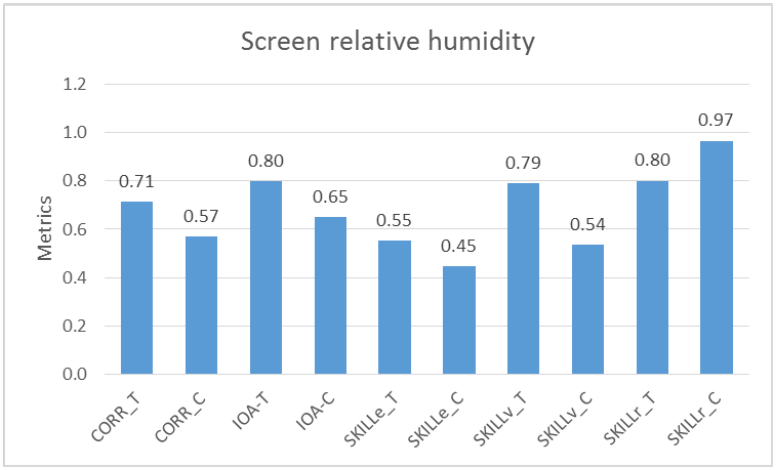

Figure 6. Statistical measures for quantitative comparison of the TAPM and CCAM screen relative humidity. T=TAPM, C=CCAM, O=Observations. Top- Mean-T, Mean-C, Mean-O; mean TAPM, CCAM and observed relative humidity. Std-T/C standard deviation of the modelled relative humidity (TAPM; CCAM), RMSE- root mean square error; RMSEs- systematic root mean square error; RMSEu- unsystematic root mean square error. Bottom- the metrics are CORR correlation coefficient; IOA- index of agreement; SKILLe = RMSEu/STD-O, SKILLv = Std-model/Std-obs, SKILLr = RMSE/Std-O.

Atmospheric soundings were undertaken at least once per day (000 UTC) for the majority of days in the period 8-21 February 2006. Sondes were released from the Cape Grim monitoring station and returned height, pressure, temperature, humidity, wind speed and wind direction data at 10-20 m intervals between the surface and about 3000 m. We have used the data to calculate potential temperature and derived the potential temperature gradient using central differences over height intervals of 30-40 m (to include some smoothing of the raw radiosonde data). The observed boundary layer heights have been diagnosed by searching for positive gradients in the potential temperature profile.

Figure 7 shows the modelled (TAPM and CCAM) hourly PBL time series with the spot hourly PBL observations superimposed on the plot. The figure is helpful because it shows the significantly hourly variability in the modelled PBL- which because Cape Grim is strongly influenced by maritime air, does not strongly follow the typical diurnal variation of PBL growth and collapse associated with sensible heating and long wave radiation cooling over land. Figure 7 suggests that both models have captured important features in the observed PBL heights, including the period of low boundary layer height between hours 168 and 264.

Figure 8 shows a scatter plot of the observed and modelled PBL heights and indicates that 71% of the TAPM PBL heights lie within a factor of two of the observed and 79% of the CCAM PBL heights are within a factor of two. This is a good result given the complexity of the observed meteorological flows at the Cape Grim monitoring station.

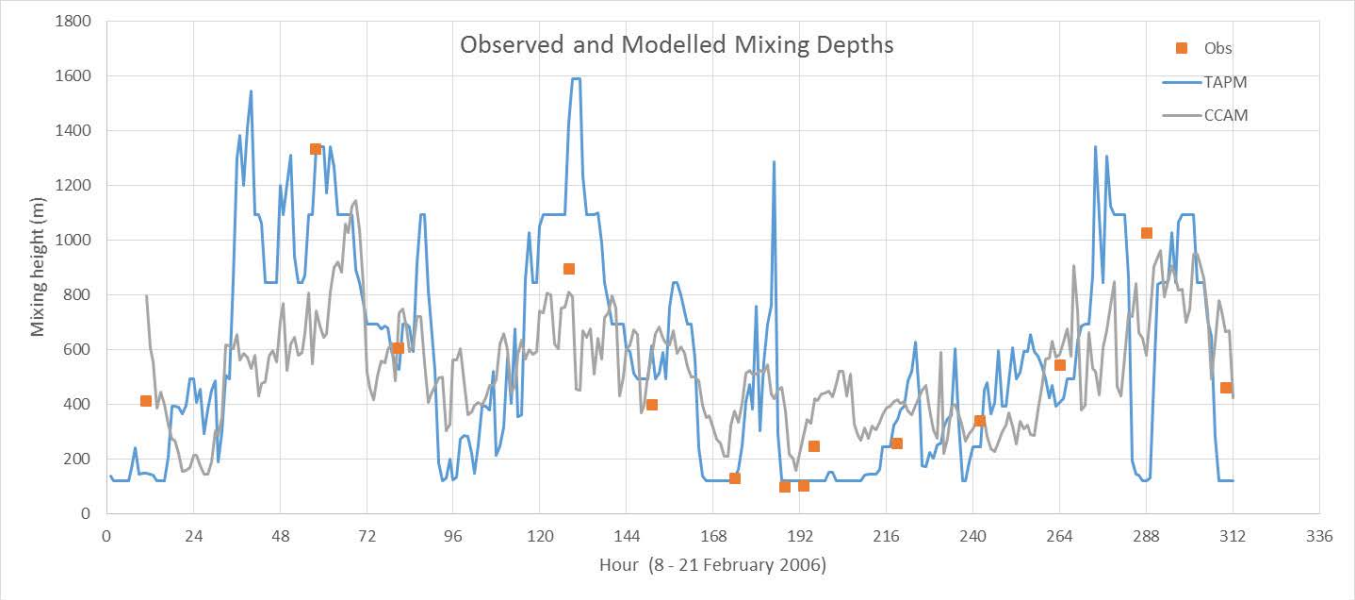

Figure 7. Hourly time series of the modelled (TAPM and CCAM) PBL heights for the period 8 – 21 February 2006. Also shown are PBL heights diagnosed from sonde data released periodically at Cape Grim during the study period.

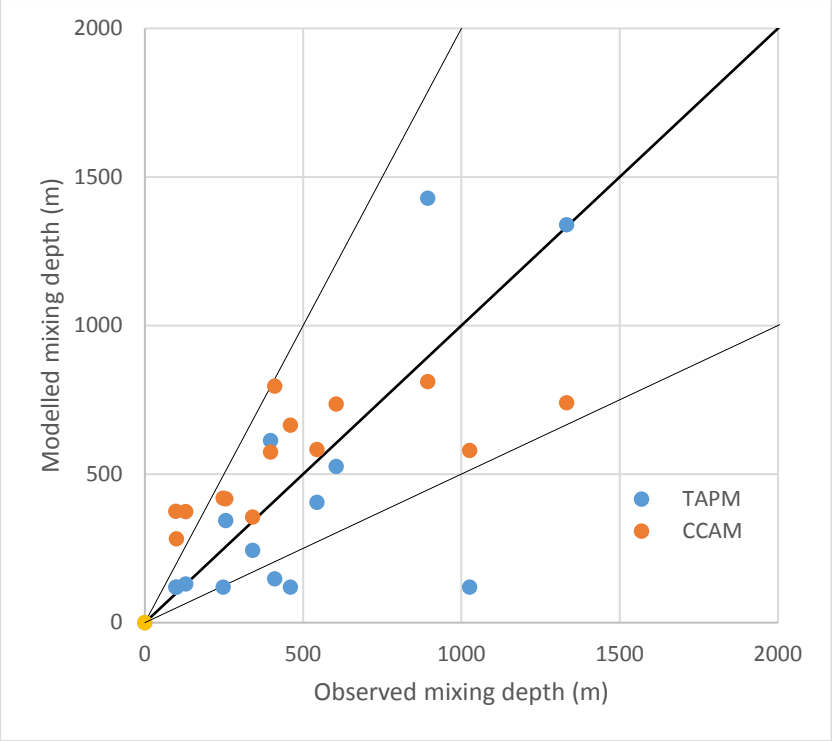

Figure 8. Scatter plot of observed and modelled PBL heights for hours corresponding to sonde releases at Cape Grim in February 2006.

Performance of TAPM-CTM for background O_3

The model generally captures background O_3 very well. The average modelled mean O_3 during background (non BB) periods was 17.7 ppb versus 16.6 ppb observed, with a coefficient of determination of 0.4. The scatter plot below (Figure 9) shows that all modelled concentrations are within a factor of 2 of observations (hourly data). Further, the campaign average diurnal 1 hour O_3 (observed vs modelled) (Figure 10) indicates maximum differences of 2 ppb (< 15% of the hourly mean).

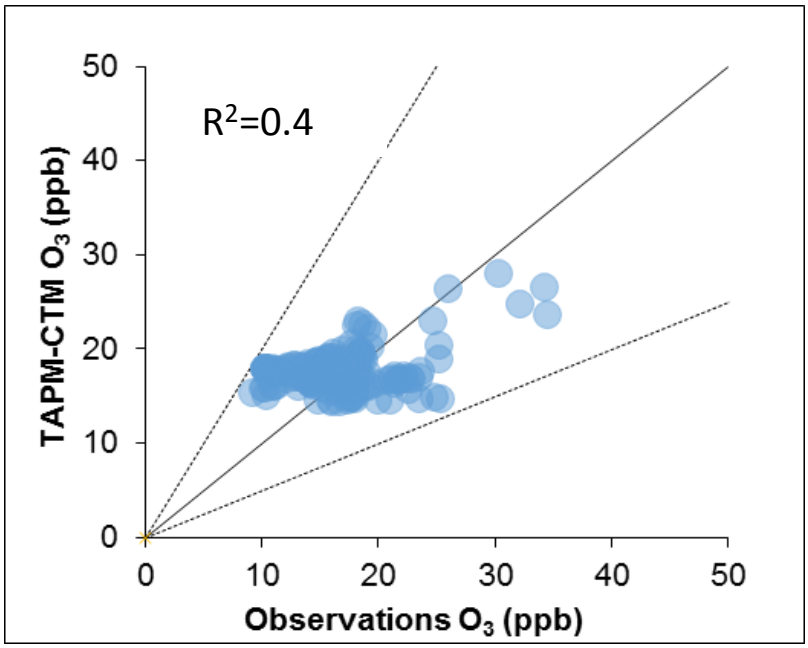

Figure 9. Hourly observed versus modelled O_3 concentrations for background (non-BB) periods

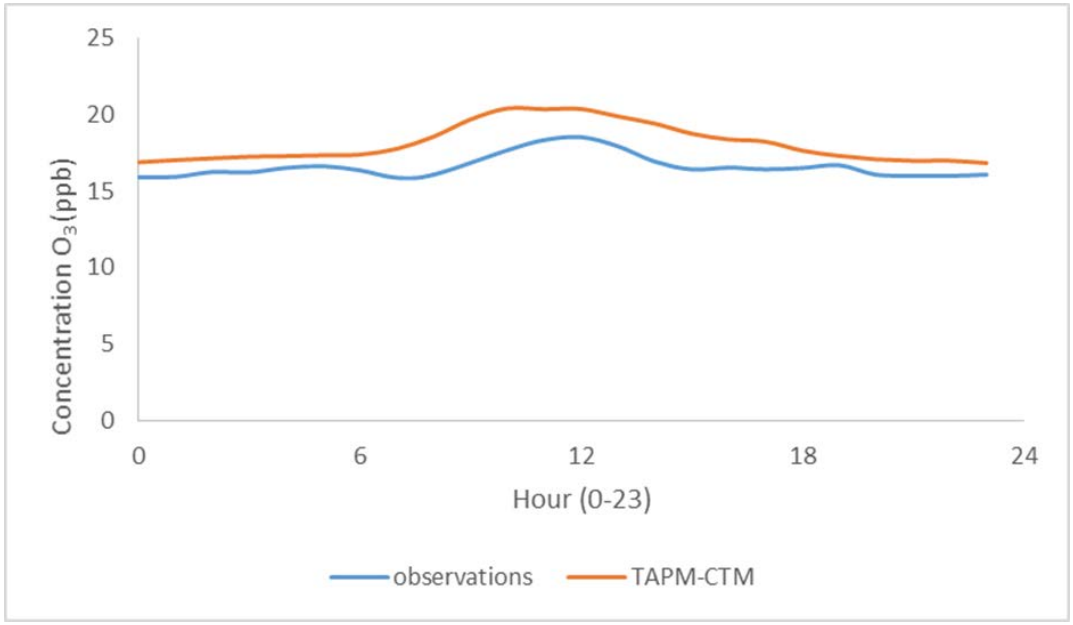

Figure 10. Dirunal observed and modelled (TAPM-CTM) concentration for background (non-BB) periods

Performance of TAPM-CTM and CCAM-CTM for different Emission Factor Scenarios

A series of qualitative and quantitative performance measures have been provided for the different EF scenarios. These measures follow the framework discussed in Dennis et al. (2010), and use the performance goals described in Boylan and Russell (2006). These measures provide quantitative evidence that the best overall agreement with the observations for both primary (EC/CO) and secondary (O_3) species is for the TAPM-CTM run with MCE = 0.89. This is discussed further below.

Quantile–quantile plots of observed and modelled BC/CO for eight model scenarios are presented in Figure 8 in the main manuscript and are not discussed further in the supplementary section.

Figure 11 and Figure 12 respectively show the mean fractional bias (MFB) and mean fractional error (MFE) of the modelled EC/CO simulations. Following Boylan and Russell (2006) we define MFB and MFE as follows.

$$MFB = 100\% \times \frac{2}{N} \sum \frac{(M_i - O_i)}{(M_i + O_i)}$$

$$MFE = 100\% \times \frac{2}{N} \sum \frac{|M_i - O_i|}{(M_i + O_i)}$$

where M_i and O_i are the i^{th} model–observation concentration pair (here coupled in time and space), and N is the number of data points. Guidance with respect to model performance is given by the criteria (outer lines) and goal (inner lines) which asymptote from a magnitude of 2.0 for EC/CO < 1.0 ng m^{-3} ppb^{-1} to 0.15 and 0.3 (MFB) and 0.35 and 0.5 (MFE) in the limit of large EC/CO (Boylan and Russell, 2006).

Figure 11 shows that the TAPM-CTM; MCE= 0.89 scenario has the smallest MFB, followed by CCAM-CTM; MCE= 0.89. Only the no-fire and MCE= 0.89 scenarios fall within the defined goal. Figure 13 shows the MFE and indicates that all of the simulations are challenged by the defined goal, while only the TAPM-CTM; MCE= 0.89 and the no-smoke scenarios fall within the defined criteria.

With respect to O_3, we analysed the entire data series (both the BB and background periods) because urban air (in non BB periods) represents a significant source of O_3 at Cape Grim, and the test of the models is to reproduce O_3 from fire as well as from other sources.

The quantile-quantile plots in Figure 9 in the main manuscript and Figure 13 show that the TAPM-CTM; MCE=0.89 scenario lies close to the 1:1 line for all of the sampled percentiles, and is in best agreement with observations. On the other hand, the MCE=0.92 and MCE=0.95 runs both for TAPM-CTM and CCAM-CTM predict depletion of O_3, an event which is not observed, as discussed in the manuscript. With the exception of these anomalous model depletion events, all modelled percentiles fall well within a factor of two of the observations.

Figure 14 shows the MFB for O_3 and indicates that the lowest MFB was for TAPM-CTM; MCE= 0.92. All but one scenario was able to simulate the one-hour O_3 with a MFB which fell within the range ±0.06. The MFB from all of the simulations fall well within the performance criteria and goal.

Figure 15 shows the MFE for O_3 and indicates that all MFE values are between 0.18- 0.29, again well with the performance criteria and goals. The MFE for TAPM-CTM; MCE=0.89 was 0.2, falling at the lower end of the MFE generating by our suite of simulations.

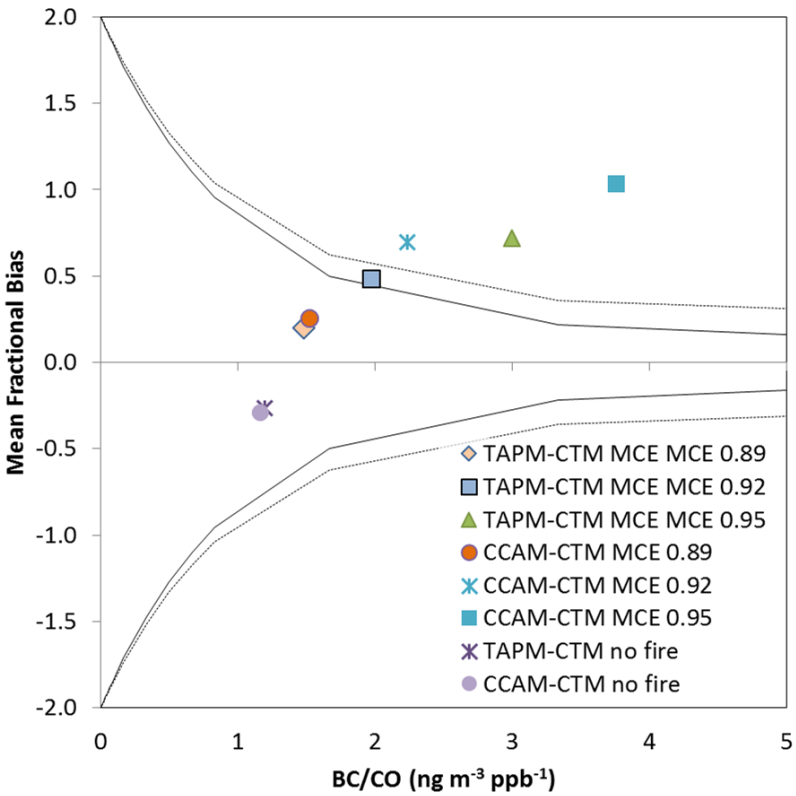

Figure 11. Mean fractional bias for BC/CO. Dotted and solid lines define the performance criteria and goal.

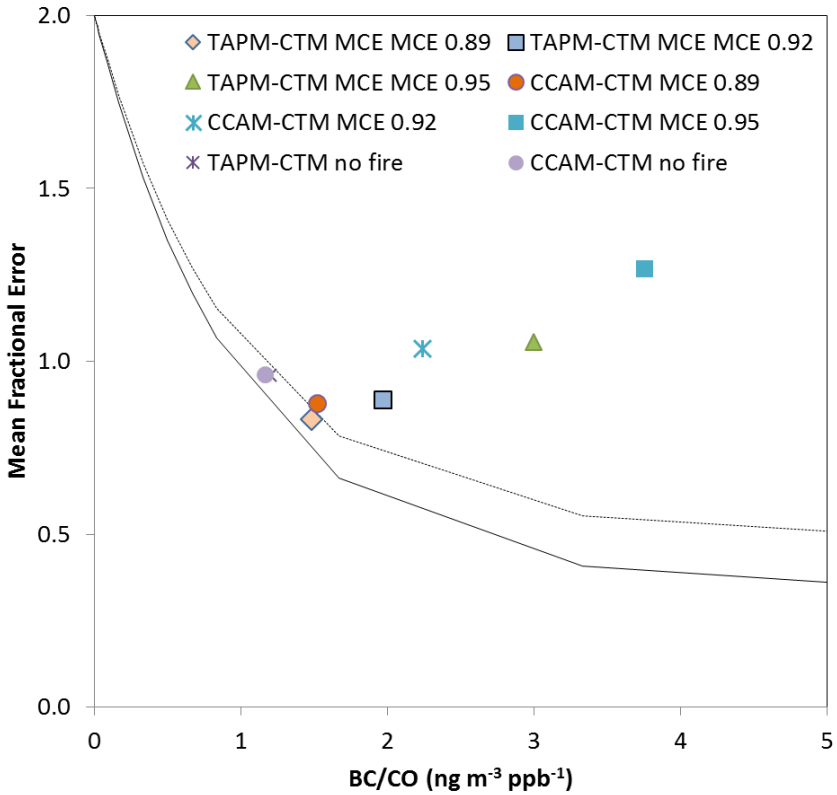

Figure 12. Mean fractional error for BC/CO. Dotted and solid lines define the performance criteria and goal.

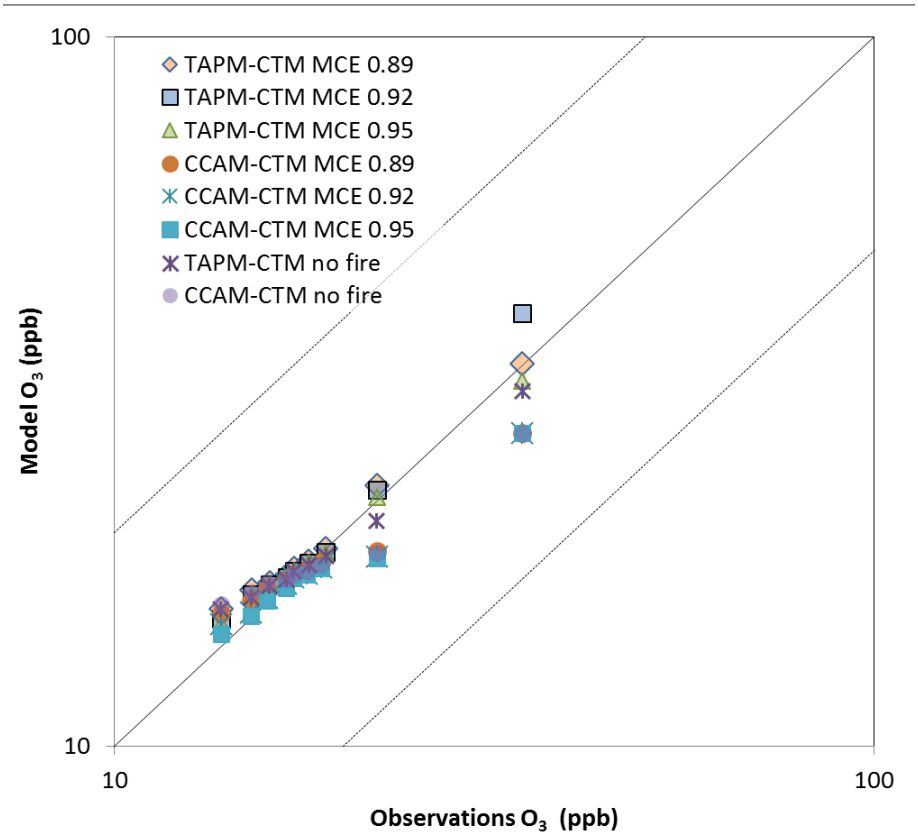

Figure 13 Quantile-quantile plots of observed and modelled O_3 for the TAPM-CTM and CCAM-CTM simulations. The plot is similar to Figure 9 in the main manuscript, but with smaller concentration range so detail can be seen.

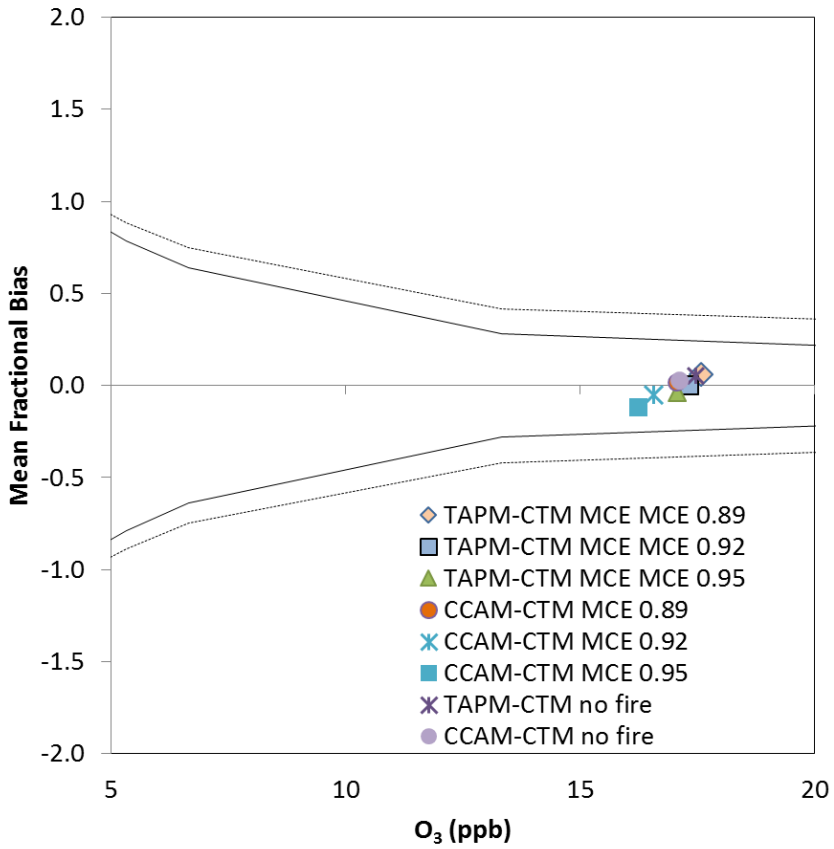

Figure 14 . Mean fractional bias for O_3. The dotted and solid lines define the performance criteria and goal.

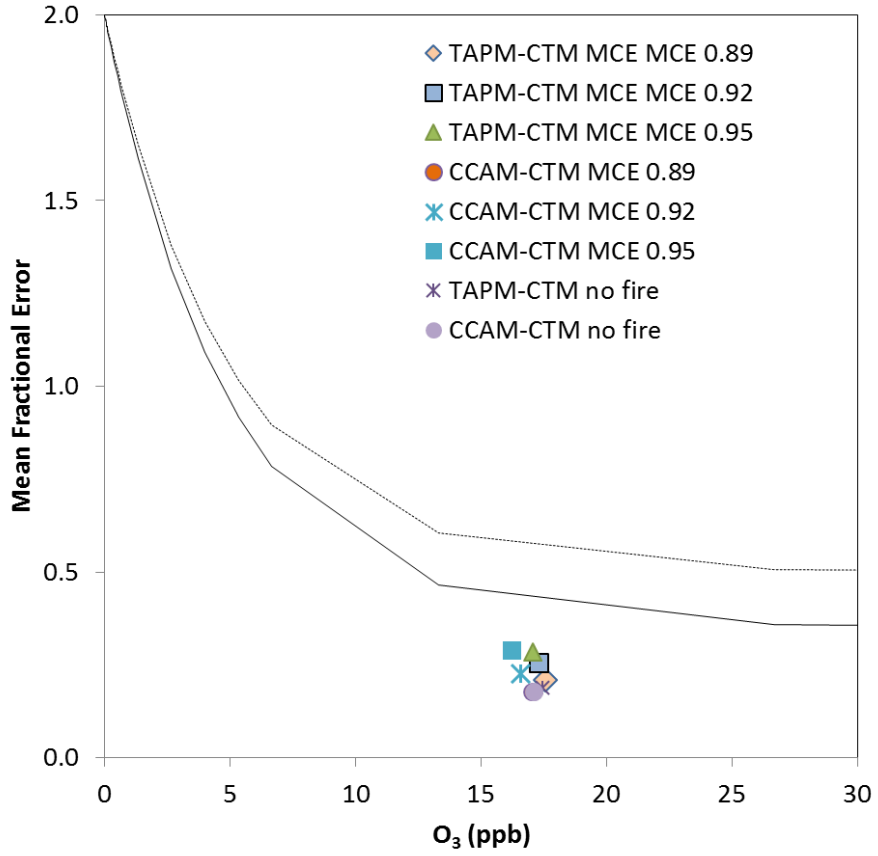

Figure 15. Mean fractional error for O_3. The dotted and solid lines define the performance criteria and goal.

In summary, the quantile-quantile plots for EC/CO (fire periods) and O_3 (all periods) demonstrate that, generally, the TAPM-CTM MCE=0.89 scenario is in best agreement with observations. This scenario also has the lowest MFB and MFE for EC/CO, and small values of MFB and MFE for O_3 which fall well within our performance criteria and goals. Additionally, this scenario did not generate the anomalous depletion of O_3 as modelled by the MCE=0.92 and MCE=0.95 scenarios.

References

Boylan, J.W., Russell, A.G., 2006. PM and light extinction model performance metrics, goals, and criteria for three-dimensional air quality models. Atmospheric Environment 40, 4946-4959.

Dennis, R., Fox, T., Fuentes, M., Gilliland, A., Hanna, S., Hogrefe, C., Irwin, J., Rao, S.T., Scheffe, R., Schere, K., Steyn, D., Venkatram, A., 2010. A framework for evaluating regional-scale numerical photochemical modeling systems. Environ Fluid Mech 10, 471-489.

Hurley, P.J., Physick, W.L., Luhar, A.K., Edwards, M., 2005. The air pollution model (TAPM) version 3. Part 2, Summary of some verification studies. CSIRO Atmospheric Research Technical Paper No. 72 . Aspendale, Victoria 3195 Australia. Available at http://pandora.nla.gov.au/tep/14280 (last accessed 28/9/2017)

Hurley P., 2008. Development and Verification of TAPM. In: Borrego C., Miranda A.I. (eds) Air Pollution Modeling and Its Application XIX. NATO Science for Peace and Security Series Series C: Environmental Security. Springer, Dordrecht,208-216.
Lawson, S. J., Keywood, M. D., Galbally, I. E., Gras, J. L., Cainey, J. M., Cope, M. E., Krummel, P. B., Fraser, P. J., Steele, L. P., Bentley, S. T., Meyer, C. P., Ristovski, Z., and Goldstein, A. H.: Biomass burning emissions of trace gases and particles in marine air at Cape Grim, Tasmania, Atmos. Chem. Phys., 15, 13393-13411, 10.5194/acp-15-13393-2015, 2015.
McGregor J.L., Dix M.R., 2008. An Updated Description of the Conformal-Cubic Atmospheric Model. In: Hamilton K., Ohfuchi W. (eds) High Resolution Numerical Modelling of the Atmosphere and Ocean. Springer, New York, NY51-75.
Thorpe, A. J. 1985. Mesoscale Meteorological Modelling By R. A. Pielke. Academic Press, 1984, Pp. 612, £55.50, US$79. Q.J.R. Meteorol. Soc., 111: 671–672. doi:10.1002/qj.49711146829
Willmott, C.J., 1981. On the Validation of Models. Physical Geography 2, 184-194.